


# Physical exercise induces structural alterations in the hippocampal astrocytes: exploring the role of BDNF-TrkB signaling

Atoossa Fahimi<sup>1,2</sup> · Mehmet Akif Baktir<sup>1</sup> · Sarah Moghadam<sup>1</sup> · Fatemeh S. Mojabi<sup>1,2</sup> · Krithika Sumanth<sup>1</sup> · M. Windy McNerney<sup>1,2</sup> · Ravikumar Ponnusamy<sup>1</sup> · Ahmad Salehi<sup>1,2</sup> 

Received: 8 July 2016 / Accepted: 9 September 2016 / Published online: 29 September 2016  
© Springer-Verlag Berlin Heidelberg (outside the USA) 2016

**Abstract** While it has been known that physical activity can improve cognitive function and protect against neurodegeneration, the underlying mechanisms for these protective effects are yet to be fully elucidated. There is a large body of evidence indicating that physical exercise improves neurogenesis and maintenance of neurons. Yet, its possible effects on glial cells remain poorly understood. Here, we tested whether physical exercise in mice alters the expression of trophic factor-related genes and the status of astrocytes in the dentate gyrus of the hippocampus. In addition to a significant increase in *Bdnf* mRNA and protein levels, we found that 4 weeks of treadmill and running wheel exercise in mice, led to (1) a significant increase in synaptic load in the dentate gyrus, (2) alterations in astrocytic morphology, and (3) orientation of astrocytic projections towards dentate granule cells. Importantly, these changes were possibly linked to increased TrkB receptor levels in astrocytes. Our study suggests that astrocytes actively respond and could indeed mediate the positive effects of physical exercise on the central nervous system and potentially counter degenerative processes during aging and neurodegenerative disorders.

**Keywords** Physical activity · Hippocampus · Dentate gyrus · *Bdnf* · GFAP · Astrocytes

## Introduction

The reciprocal relationship between body and mind has been the subject of an intense investigation for centuries (see for review Phillips et al. 2014). While multiple aspects of CNS functions including arousal, attention, decision-making, executive function, and learning and memory have shown to improve due to physical exercise (PE) (Marlatt et al. 2012; Salis 2013; Scarmeas et al. 2009, 2011), only recently the exact mechanisms behind the relationship between PE and higher-level brain functions are becoming elucidated. In addition to improving normal physiology, it appears that PE can impose disease-modifying effects in several neurodegenerative disorders, particularly Alzheimer's disease (AD) (see Phillips et al. 2015a). Indeed, it has been shown that PE can lead to a number of beneficial and preventative effects in AD patients (for review see Phillips et al. 2015a). Individuals who engaged in mentally and physically demanding activities have a fourfold reduction in the risk of developing dementia of AD type (Barnes and Yaffe 2011). Based on this, it has been estimated that a 25 % increase in PE could potentially reduce the prevalence of AD by 1 million worldwide (Barnes and Yaffe 2011). Despite all these, the neurobiological basis of the relationship between PE and neurodegeneration remains to be fully understood. Indeed, elucidating the exact mechanisms behind the effects of PE on the CNS would potentially lead us to new therapeutic strategies for neurodegenerative disorders including AD.

The most widely studied effects of PE on the CNS include the release of trophic factors and enhanced

---

A. Fahimi and M. Akif Baktir contributed equally to this work.

**Electronic supplementary material** The online version of this article (doi:10.1007/s00429-016-1308-8) contains supplementary material, which is available to authorized users.

---

✉ Ahmad Salehi  
asalehi@stanford.edu

<sup>1</sup> VA Palo Alto Health Care System, 3801 Miranda Ave, Palo Alto, CA 94304, USA

<sup>2</sup> Department of Psychiatry and Behavioral Sciences, Stanford University School of Medicine, Palo Alto, CA 94304, USA

neurogenesis in the dentate gyrus (DG) of the hippocampus (Cotman et al. 2007; van Praag 2008). Here, we assessed the effects of PE on astrocytes, i.e. the most abundant cell type in the brain, which, play a significant role in synaptic transmission, and the uptake of glutamate from the synaptic milieu. Furthermore, through reactive astrogliosis, astrocytes respond to CNS injury by reversible gene expression along with astrocytic hypertrophy (Sofroniew and Vinters 2010). Strategically located with their extensive projections, astrocytes constitute the third element (the pre and postsynaptic neurons constitute the other two) of the synaptic structure and induce a bi-directional influence on the synaptic function (Filous and Silver 2016). Furthermore, these cells play a significant role in the maintenance of blood brain barrier (BBB), which seems to be compromised in AD (Gosselet et al. 2013).

A number of studies suggest that the synthesis and release of trophic factors particularly brain-derived neurotrophic factor (Bdnf) play a crucial role mediating the effects of PE on the CNS (Vaynman et al. 2004; Nascimento et al. 2015; Moretti et al. 2009). Indeed, PE can lead to a significant increase in *Bdnf* gene expression in the hippocampus (Neeper et al. 1996). Astrocytes are able to respond to Bdnf through expressing both full length and truncated tropomyosin receptor kinase B (TrkB) receptors (Ohira et al. 2005; Aroeira et al. 2015).

As we report here, long-term PE in mice led to a significant increase in the synthesis and release of Bdnf along with an alteration in the morphology of astrocytes in the DG. Importantly, our data suggest that these effects are mediated through Bdnf-TrkB signaling. The functional significance of morphological alterations will be discussed.

## Materials and methods

### Animals

Six pairs of adult (5–6 months) male *C57BL/6* (stock number: 000664) mice were used for all the experiments. The mice were obtained from the Jackson Laboratory, Bar Harbor, ME and shipped at 3 weeks of age to our facility. All mouse experiments were approved by the Committee on Animal Research at the Veterans Affairs Palo Alto Health Care System (VAPAHCS). All animals were group-housed at the VAPAHCS on a 12-h light/dark cycle in a temperature- and humidity-controlled environment, with ad libitum access to food and water. The mice were randomly divided into two groups of exercise (EX) and non-exercise (non-EX).

### The physical exercise protocol

Adult mice were exposed to a combination of treadmill and running wheel (to achieve the maximum effects) or sham treatment. The running wheels were placed in the home cages to avoid stress. The entire protocol lasted 5 weeks. During the first week, all mice were habituated by daily handling. Starting from the 2nd week of the training, all mice (EX and non-EX) were placed for 30 min in the proximity of a treadmill machine for further habituation prior to treadmill exercise. The treadmill device (Treadmill Simplex II, Exer-6M, Columbus Instruments) consists of six parallel tracks angled at 0° allowing simultaneous running (Fig. S1A). Thereafter, each EX mouse was placed on the treadmill machine for 5 min after which, the tracks started moving (8 meter (m) /min) for two cycles of 20-min each with a 10-min break in between per day (5 days per week). In case that the mice did not move, their tail would touch a well-cushioned wall behind them. A combination of a habituation period in the treadmill and the use of well-cushioned walls behind the mice was used to minimize the amount of possible stress. The speed of treadmill was escalated on the following weeks by 2 m/min per week for 4 consecutive weeks (8, 10, 12, and 14 m/min for weeks 2–5, respectively) (Fig. S2B).

### Postmortem analysis

At the end of the last day of the protocol, all EX and non-EX mice were deeply anaesthetized using intraperitoneal (IP) injection of ketamine (60 mg/kg) and xylazine (12 mg/kg) (Leiter's Compounding Pharmacy, CA), followed by transcardial perfusion with ice-cold saline, and the brain was extracted.

### Brain sample preparation

Following brain extractions, the left hemispheres were flash frozen in liquid nitrogen for gene expression studies (real time qPCR), and ELISA. The right hemispheres were fixed in 4 % buffered paraformaldehyde (Sigma-Aldrich) overnight at 4 °C followed by dehydration in 30 % sucrose (Sigma-Aldrich) and freezing on dry ice. This was followed by embedding each brain in optimum cutting temperature (OCT; Sakura) and storing at –80 °C. For ELISA, the DG region was micro-punched. Under a dissection microscope (Evolution × R6), the DG of hippocampal regions were dissected out and micro-punched with a needle (Uni-Core-0.35) at –21 °C in a cryostat (Leica CM 1950), and stored at –80 °C (Dang et al. 2014). It has been shown that the neighboring regions around the micro-punch zone contain minimal amounts of Bdnf (Hofer et al. 1990).

## ELISA

The micro-punched samples (4–5 on average) from individual mice were mixed in 1 ml of lysis buffer, sonicated on ice followed by centrifugation at 16,000g for 30 min according to Pollock and colleagues (Pollock et al. 2001). The pellets obtained following centrifugation was stored at  $-80^{\circ}\text{C}$  for total protein levels quantification. The protein levels were quantified using a micro BCA protein assay kit (23235, Thermo Scientific) and a spectrophotometer (Fisher Scientific Multiskan) with absorbance measured at 562 nm. An ELISA kit (Boster Life Sciences, Mouse Bdnf PicoKine™ ELISA Kit EK0309) was used for Bdnf quantification according to the manufacturer's recommendations. The ELISA results were detected using Multiskan spectrophotometer (Song et al. 2016).

## PCR array

Fifty mg of tissue from the hippocampus of an EX mouse and a non-EX mouse was homogenized and the total RNA was isolated using TRIzol Reagent (Invitrogen). The RNA was further purified using RNeasy Mini Kit (Qiagen) and quantified with a NanoDrop ND-1000 spectrophotometer (Thermo Scientific). First strand cDNA was then synthesized from 500 ng of the total RNA using RT<sup>2</sup> First Strand Kit (Qiagen). Gene expression was then performed using the 96-well format mouse neurotrophin and receptor RT<sup>2</sup> Profiler PCR Arrays (PAMM-031Z; Qiagen) according to the manufacturer's protocol. The Agilent Technologies Mx3005P system was used for qPCR and the results were analyzed using the RT<sup>2</sup> Profiler PCR array data analysis tool (Qiagen). This array enabled us to profile the expression of 84 genes including trophic factor-related molecules and used five housekeeping genes as normalizers (Table S1).

## Immunocytochemistry

The brain samples were coronally cut (70- $\mu$ -thick) using a cryostat and placed in cryoprotectant solution (25 % ethylene glycol, 25 % glycerol and 0.05 M sodium phosphate buffer, pH = 7.4), and stored at  $-20^{\circ}\text{C}$  till use.

## GFAP staining

Seventy-micrometre-thick floating sections throughout the entire septo-temporal extent of the hippocampus were washed with tris-buffered saline (TBS), pre-incubated with 0.3 % triton, and 10 % normal horse serum (NHS) in TBS for 1 h at room temperature (RT) prior to immunostaining. Two sets of sections (for light and fluorescent microscopy) were then incubated for 3 h in RT then overnight at  $4^{\circ}\text{C}$

using a goat antibody against GFAP (glial fibrillary acidic protein) (1:200; Abcam, ab53554) diluted in 1 % NHS and 0.3 % triton in TBS. This antibody has been raised against a synthetic peptide corresponding to C terminal amino acids of human GFAP (DGEVIKESKQEHKD, 417–430) and used extensively to image astrocytes in rodents (Liu et al. 2012) and it recognizes a single band in the Western blot analysis of the mouse brain (Jeong et al. 2015). The sections were washed for 5 min, three times in TBS. The primary antibody was followed by incubation with a biotinylated-s-conjugated horse anti-goat IgG (1:200; Vector Lab, BA-9500) for 1 h at RT. The sections were washed for 5 min, three times in TBS. For the light microscopy, the sections were incubated in VECTASTAIN ABC Lite (1:1000; Vector Lab) for 1.5 h at RT followed by incubating sections in DAB and cover-slipping using DPX mountant. In the fluorescent set, the reaction continued by incubating sections in Texas red streptavidin (1:200, Vector Lab, SA-5006) for 1 h at RT and washed for 5 min three times in TBS then cover-slipping using fluorescent Vectashield (Vector Lab) mountant.

## GFAP-TrkB double staining

Floating sections throughout the entire hippocampus were washed in TBS, pre-incubated with 0.3 % triton, and 10 %

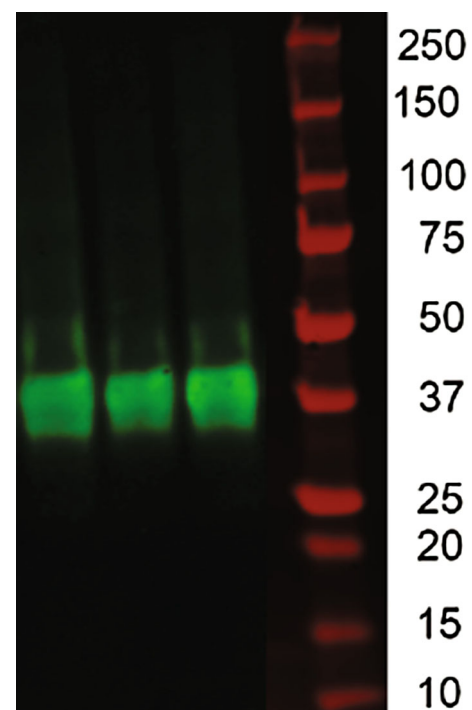


**Fig. 1** Western blot of mouse brain homogenates from three mice stained using a rabbit monoclonal antibody raised against the C terminus of human synaptophysin (SP11). A  $\sim 37$ -kDa band was detected corresponding to the mouse synaptophysin

NHS in TBS for 1 h at RT prior to immunostaining. The sections were then incubated for 3 h in RT then overnight at 4 °C using a goat antibody against GFAP (1:200, Abcam, ab53554) and a rabbit antibody against TrkB (1:2500, Millipore, AB5372) diluted in 1 % normal goat serum (NGS) and 0.3 % triton in TBS. The pan-TrkB antibody has been raised against a recombinant protein from the extracellular domain of rat TrkB (aa. 54–67) and specifically recognizes both truncated and non-truncated TrkB molecules (Helgager et al. 2014). The incubation with primary antibodies was followed by washing for 5 min, three times in TBS then incubated with a biotinylated-s-conjugated horse anti-goat IgG (1:200, Vector Lab, BA-9500) for 1 h at RT. The reaction was followed by 5 min wash (three times) in TBS and incubating sections in Texas red streptavidin (1:200, Vector Lab, SA-5006) and fluorescein goat anti-rabbit IgG antibody (1:200, Vector Lab, FI-1000) for 1 h at RT. The sections were washed for 5 min, three times in TBS and cover-slipped using Vectashield. No immunoreactivity was found in control sections omitting the primary antibodies. In our control studies, the secondary antibody of TrkB (fluorescein goat anti-rabbit IgG) did not react with the primary anti-GFAP antibody and vice versa.

### Synaptophysin

To label presynaptic densities, a rabbit monoclonal antibody (SP11, Spring Bioscience, M3114) was used to label synaptophysin. The antibody recognizes a 38-kDa molecule corresponding to the C terminus of human synaptophysin. Seventy-micrometre-thick floating sections were washed in TBS then pre-incubated with 0.5 % triton, 5 % milk, and in TBS for 1 h at RT prior to immunostaining. The sections were then incubated for 1 h at RT using SP11 to label synaptophysin, diluted in 0.5 % triton, 5 % milk, and in TBS for 1 h in RT then 24 h in 4 °C. The reaction was followed by a wash for 5 min three times in TBS, then continued with incubation with DyLight 488 horse anti-rabbit IgG antibody (1:200, Vector Lab, DI-1088) for 1 h at RT. The sections were washed for 5 min three times in TBS and cover-slipped using Vectashield.

### Western blotting

SP11 antibody has shown to be a very sensitive antibody for detection of synaptophysin (Rossi et al. 2005). To test the specificity of the antibody, tissue samples from a mouse brain homogenates were used for western blotting using the SP11 antibody (Fig. 1). Brain samples were homogenized in RIPA buffer containing a tablet of protease inhibitors (cOmplete Uitra Tablets, Mini, with EDTA, EASYpack, Life Science, 05892970001) along with a table of

phosphatase inhibitor (EASYpack foil blister, Life Science, 0490684500). Approximate protein concentration was quantified using NanoDrop ND-1000 spectrophotometer (Thermo Scientific) and samples were diluted with buffer and about 2–5 µg of total protein was loaded into each well. Before loading, samples were diluted 1:5 in Western loading buffer (Invitrogen) and 1:40 in mercaptoethanol. They were then boiled at 90 °C for 2 min followed by centrifugation at 13000 rpm at 4 °C for 4 min. Each sample was loaded into 4–20 % precast polyacrylamide gels (Biorad). Eight microliters of the ladder (Odyssey, 928-40000) was also loaded in a different well. Electrophoresis was run in tris-glycine buffer containing 1 % SDS (Biorad) at 100 V for 1 h, or until the loading buffer reached close to the bottom of the gel. Protein transfer onto nitrocellulose membrane (Biorad) was carried out at 70 V for 2 h in tris-glycine buffer (Armresco) containing 5 % methanol. The membranes were then incubated in fluorescent Western blocking buffer (Rockland) for 1 h at RT and rinsed with TBS buffer containing 0.5 % tween. Membranes were incubated separately in primary antibody (SP11, 1:1000) overnight at 4 °C. After an extensive wash in a buffer, membranes were incubated in secondary fluorescent antibody IRDye 800CW goat anti-rabbit IgG (H + L) (Licor, 1:1200, 926-3221) for 1 h at RT. The blot was imaged on the Odyssey imaging system at 800CW (Fig. 1).

### Morphometry and image analysis

#### *Astrocytes number and morphology*

The total number of astrocytes in the molecular layer (ML) of the DG was determined using systematic random sampling using Stereoinvestigator (MBF Bioscience) in 100X objective images throughout the entire septo-temporal axis of the hippocampus (on average 6–7 coronal sections). On average  $1028 \pm 236$  (mean  $\pm$  SD) astrocytes per mouse in the EX group and  $779 \pm 104$  astrocytes per mouse in non-EX group were used to estimate the total number of astrocytes. Separately, using Neurolucida (MBF Bioscience), the location and the extent of astrocytic projections were determined in 100X objective images. This was done by manual tracing of individual projections of all astrocytes in the ML in coronal sections throughout the entire septo-temporal extent of the DG. The total length of processes along with the surface area (the area generated by enclosing a polygon that connects the most distal points of processes in a tree) were calculated (see Das et al. 2015 for details). Neurolucida was also used to assess the orientation of astrocytic projections in each section. It has been shown that in the dentate gyrus, nearly all cells in stratum granulosum are mRNA-positive and Bdnf-immunoreactive (Bdnf-Ir). Furthermore, in the ML, a laminar

pattern of Bdnf-Ir has been seen with highest levels of Bdnf Immunostaining in the inner ML and the lowest in the outer ML (Kokaia et al. 1995). The users were blinded to the treatment in the entire study. To determine the distance among astrocytes, the shortest distance between neighboring cell bodies was quantified.

### Colocalization analysis

Using both TrkB and GFAP images, the total area covered by TrkB was quantified in GFAP-positive profiles (Image Pro Plus, Media Cybernetics). Around 50 images were randomly selected from the ML using Keyence (BZ-X710) digital microscope (each containing on average 2–3 astrocytes). The colocalization was performed by separately collecting images using red and green channels and superimposing them using Image Pro Plus. Following automatic background correction and deconvolution, the total number of pixels stained in both images was calculated and divided by the total number of pixels per image as a measure of colocalization. A similar process has been utilized before for colocalization (Sepulveda-Falla et al. 2011; Quirie et al. 2012).

### Synaptophysin

To examine synaptic load in the DG of the hippocampus, we examined the overall optical density of immunostaining for synaptophysin. Using a digital microscope Keyence, a total of 500 images were automatically captured from the ML of the DG using a 60X objective. Image Pro Plus was used to perform deconvolution and the quantification of the area of a mask that covered synaptophysin immunoreactivity in each image. For quantification purposes, using a statistical program (Statistica 6.0, StatSoft), a random number of measures were chosen from a pool of measurements from all the mice.

### Data analysis

All data are presented in terms of mean  $\pm$  standard error of the mean (SEM). The normality of data was tested using the Shapiro–Wilks test. The Student *t*- and non-parametric Mann–Whitney tests were used to compare the means between the two groups of EX and non-EX (Statistica). The Chi-square test was used to compare the histograms. Differences were considered to be statistically significant when  $p < 0.05$ .

## Results

The mice in this experiment underwent 4 weeks of daily exercise using a combination of intermittent treadmill (5 days per week) and free access to running wheels

(7 days per week) in their home cages. The treadmill allowed simultaneous exercise in multiple mice with limited handling and stress to the mice (Fig. S1A, B).

### PCR array

We started this investigation by quantifying the expression of trophic factor gene/s, which undergo significant alterations due to chronic PE. PCR array analysis was utilized to analyze the expression of neurotrophic factors in the hippocampus of EX mice compared with non-EX mice. Among 84 genes studied (see Table S1) trophic factors with highest increase in expression included *Bdnf* and fibroblast growth factor 2 (*Fgf2*). Indeed, there was more than fourfold increase in the expression of both trophic factors in the hippocampus of EX mice.

### Synaptic plasticity

The number of synapses in the CNS is a reliable corresponding measurement of cognitive function (Vaynman et al. 2004). To examine whether long-term PE in mice increased synaptic load, we quantified the synaptic load (% of the image covered by presynaptic synaptophysin marker, SP11-immunoreactive (Ir) in the ML of the DG in EX and non-EX mice. Chi-square test showed a significant shift in synaptic load to higher values in EX mice compared with non-EX mice ( $\chi^2 = 107.59$ ,  $df = 3$ ,  $p < 0.001$ , Fig. 2).

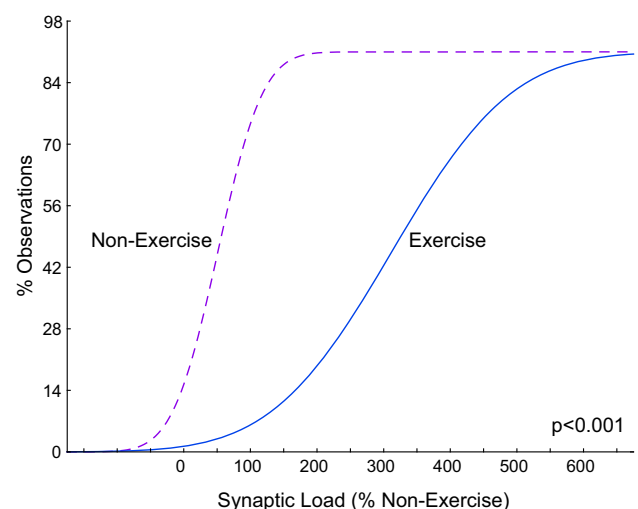


**Fig. 2** The cumulative frequency distribution of synaptic load in EX and non-EX mice.  $\chi^2$  test showed a significant shift to higher values in exercise mice compared with non-EX mice ( $p < 0.001$ )

## ELISA for Bdnf

Based on PCR array analysis, *Bdnf* and *Fgf2* showed significant increase in mRNA levels following chronic exercise. To test whether increased gene expression for *Bdnf* can be translated into elevated levels of Bdnf protein, we quantified the total levels of Bdnf in micro-punches through the DG using ELISA (Fig. 3a). The non-parametric Mann–Whitney test showed a significant increase in Bdnf levels in EX mice compared with the control group ( $p = 0.038$ , Fig. 3b).

## Morphometrical analyses

Both mRNA and protein levels for Bdnf were increased in the DG of mice undergoing exercise. To assess the effects of Bdnf on astrocytes, we performed a series of morphometrical analyses on these cells. Immunocytochemical visualization of GFAP revealed a large number of astrocytes in all three layers of the DG [dentate granule cell layer (DGCL), polymorphic layer (PML), and (ML)] (Fig. 4a, b). Using stereological methods (Salehi et al. 2006, 2009), we quantified the total number of astrocytes throughout the entire extent of the ML of the DG. No significant differences were found either in the total volume of the region (EX =  $889,660,200 \pm 46,263,333 \mu\text{m}^3$ ,  $n = 5$ , non-EX =  $773,214,800 \pm 76,596,762 \mu\text{m}^3$ ,  $n = 5$ ,  $p = 0.310$ ) or the number of astrocytes within the ML of the DG (EX =  $169,129 \pm 17,828$ ,  $n = 5$ , non-EX =  $152,916 \pm 8124$ ,  $n = 5$ ,  $p = 0.548$ ).

In addition to the total number of astrocytes, we also studied the average distance among astrocytes and the distance within the neighbors. No significant differences

were found in the average distance among astrocytes ( $p = 0.792$ , Fig. 5a) along with distance with nearest ( $p = 0.329$ , Fig. 5b) or farthest neighbors ( $p = 0.429$ , Fig. 5c). While there were no significant differences in the total number or the distance among astrocytes between the two groups, the Mann–Whitney test showed a significant increase in total length of astrocytic projections (EX =  $1023 \pm 27.1 \mu\text{m}$ ,  $n = 5$ , non-EX =  $906 \pm 11.9 \mu\text{m}$ ,  $n = 6$ ,  $p = 0.006$ ) and the surface area [EX =  $2231 \pm 83.3 \mu\text{m}^2$ ,  $n = 5$ , non-EX =  $2020 \pm 49.60 \mu\text{m}^2$ ,  $n = 6$ ,  $p = 0.028$  (Fig. 6a, b)].

As showed above, PE led to significant increase in the amount of Bdnf in the DG of the hippocampus. The question was whether the synthesis and propagation of Bdnf in the surrounding tissues would also alter the orientation of astrocytic projections. A polar histogram of the orientation of astrocytic projections showed alterations in the orientation of projections. Indeed majority of projections were found to be oriented toward the  $0^\circ$  (i.e. DGC) in EX mice (Fig. 7).

## TrkB and GFAP

Astrocytes also synthesize Bdnf and contain TrkB receptors (Schwartz and Nishiyama 1994; Zafra et al. 1992; Miklic et al. 2004). We found a significant increase in Bdnf protein levels in the DG of EX mice. The question was whether long-term production of Bdnf in EX mice could also alter TrkB expression in these cells. Using a pan-TrkB antibody, we found a significant increase in TrkB levels in GFAP-positive profiles in EX mice. Since there was no sufficient number of sections available for two cases, therefore, they were excluded from the analysis. While we

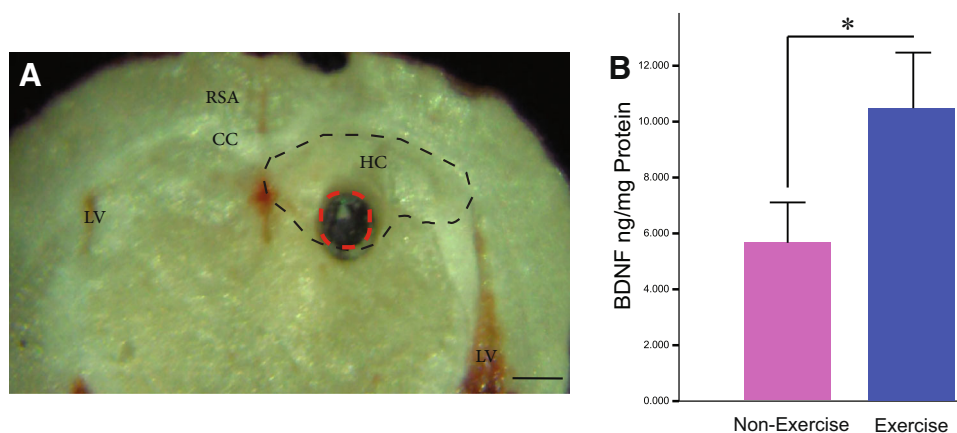


**Fig. 3** **a** Performing a micro-punch through the dentate gyrus provided enough sample to enable us to quantify Bdnf protein levels in both groups of EX and non-EX mice. Three hundred-micrometre-thick sections were cut and placed on a hard surface. 1–2 punches were done through the DG in each mouse. The collected punches were placed in a tube and stored at  $-80^\circ\text{C}$ . **b** Quantifying Bdnf

protein levels showed a significant increase in mice undergoing exercise (EX =  $10.47 \pm 1.98 \text{ ng/mg}$ ,  $n = 6$ , non-EX =  $5.62 \pm 1.42$ ,  $n = 6$ , Mann–Whitney test,  $*p = 0.038$ . CC corpus callosum, HC hippocampus, RSA retrosplenial agranular, LV lateral ventricle, scale bar 120  $\mu\text{m}$ )

**Fig. 4** **a** Photomicrograph of the dentate gyrus in the hippocampal region stained using an antibody against GFAP. Astrocytes were labeled in all three layers of the DG including polymorphic layer (PML), dentate granule cell layer (DGCL) and the molecular layer (ML). **b** Extensive astrocytic projections were observed in the DGCL. Scale bar for *a* = 50  $\mu\text{m}$  and *b* = 100  $\mu\text{m}$

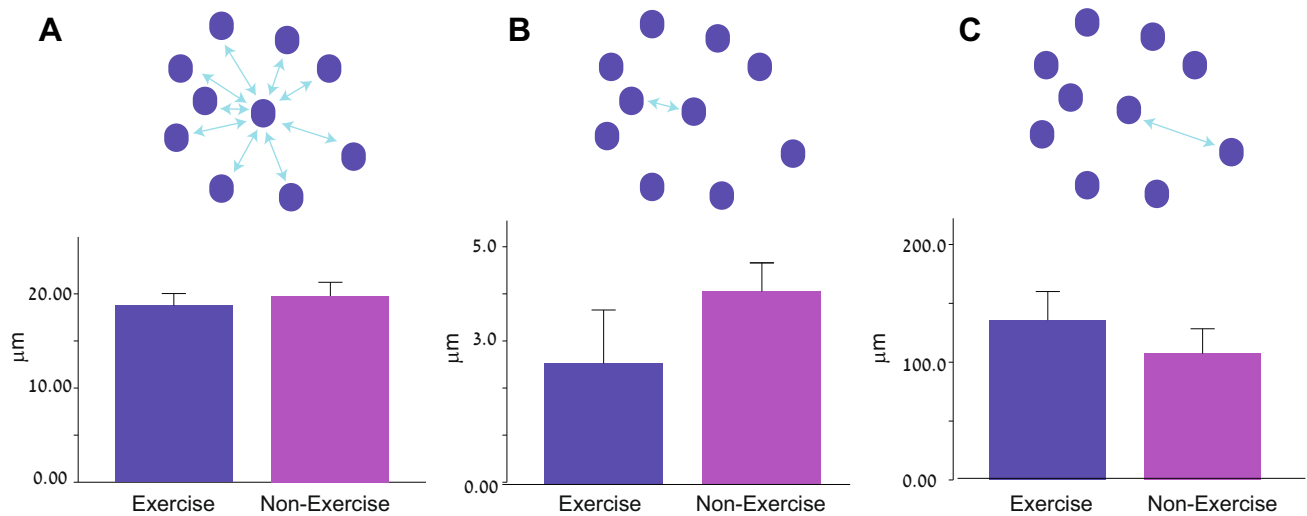
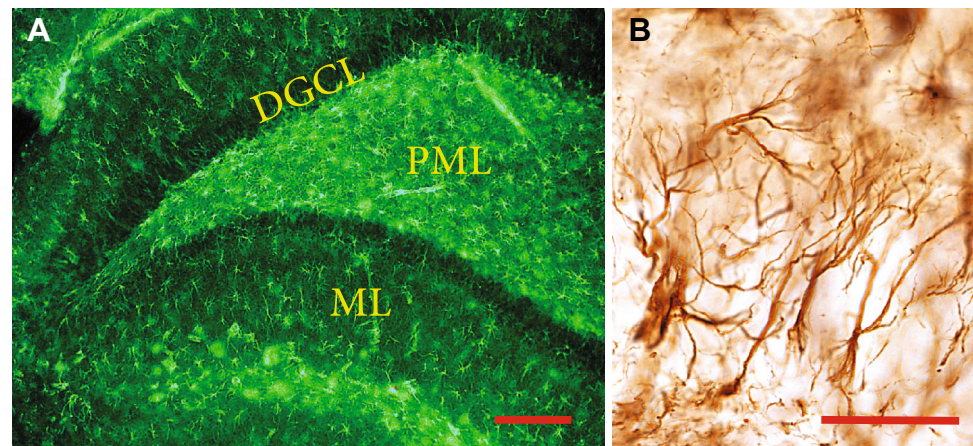


**Fig. 5** The average distance among astrocytes in the molecular layer in mice undergoing exercise. We found no significant differences in the values for the **a** average distance (non-EX =  $19.76 \pm 1.46$ ,  $n = 6$ , EX =  $18.76 \pm 1.27$ ,  $n = 5$ ,  $p = 0.792$ ) among all astrocytes, **b** the distance with nearest neighbor among astrocytes in each section

(non-EX =  $4.05 \pm 0.6$ ,  $n = 6$ , EX =  $2.52 \pm 1.1$ ,  $n = 5$ ,  $p = 0.329$ ) and **c** the distance with farthest neighbor among astrocytes in each sections (non-EX =  $107.26 \pm 21.13$ ,  $n = 6$ , EX =  $135.68 \pm 24.34$ ,  $n = 5$ ,  $p = 0.429$ )

found only a trend toward increased levels of total TrkB immunoreactivity in the DG of EX mice (non-EX =  $100.00 \pm 5.8$ ,  $n = 4$ , and EX =  $123.44 \pm 8.05$ ,  $n = 6$ ,  $p > 0.05$ ), we found a significant increase in TrkB levels in astrocytes (non-EX =  $100 \pm 10.8$ ,  $n = 4$ , EX =  $137.46 \pm 10.8$ ,  $n = 6$ ,  $p = 0.038$ ) (Fig. 8a, b).

## Discussion

In this study, we found that long-term PE in mice led to a significant increase in *Bdnf* mRNA and protein levels along with elevated synaptic load in the DG region. In addition, augmented *Bdnf* levels in the DG of EX mice led to a significant alteration in astrocytic morphology and TrkB levels in astrocytes.

Numerous studies have reported a robust relationship between PE, hippocampal size, and cognitive measures. Studies in the elderly have revealed a direct correlation between increased levels of PE and improved cognition along with an increase in hippocampal volume (Erickson and Kramer 2009). The beneficial effects of PE on the hippocampal region are thought to be mediated through improvement of neurogenesis (Yang et al. 2015), maturation of newborn neurons, as well as increased dendritic complexity and the length of dendritic spines (Cotman et al. 2007; Voss et al. 2013; Stranahan et al. 2007; Chowdhury et al. 2014).

There is a large number of published studies on the positive effects of PE on the nervous system (see Phillips et al. 2014). These positive effects are not limited to improving physiological processes but also could mitigate

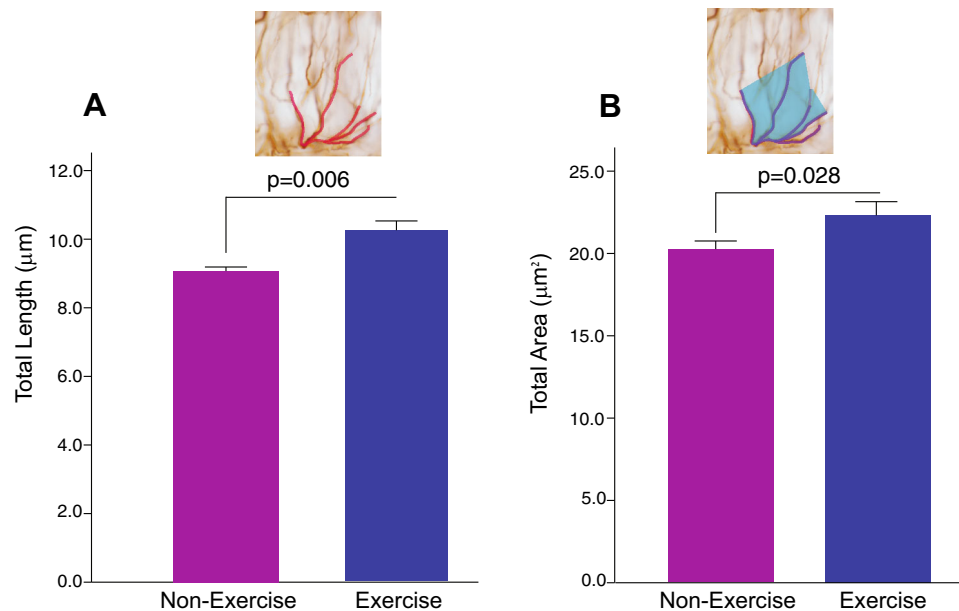


**Fig. 6** The effects of exercise on average length and the area enclosed by astrocytic projections. The Mann–Whitney test showed a significant alteration **a** in total length of astrocytic projections (EX = 10.23 ± 0.271 mm,  $n = 5$ , non-EX = 9.06 ± 0.119 mm,  $n = 6$ ,  $p = 0.006$ ). **b** A 2D images depicting surface area enclosed

by astrocytes' projections (EX = 22.31 ± 0.833 mm<sup>2</sup>,  $n = 5$ , non-EX = 20.20 ± 0.496 mm<sup>2</sup>,  $n = 6$ ,  $p = 0.028$ ). The determination of the area and surface was done in  $x$ ,  $y$ ,  $z$  planes. However, for demonstration purposes, only the  $x$  and  $y$  planes are shown here

neurodegenerative alterations in a number of neurodegenerative disorders particularly AD (Phillips et al. 2015b). The primary target for PE in the CNS is the hippocampal region, particularly the DG (van Praag 2008). Both the dendritic spine density (Zhao et al. 2006) and the rate of neurogenesis have been shown to improve in this region following PE (van Praag 2008). While the exact mechanisms behind these morphological effects remain obscure, it appears that increased synthesis and availability of neurotrophins particularly Bdnf play a role in this process (Nijs et al. 2015). We found chronic PE led to a significant shift in the frequency distribution of synaptic load to higher values (Fig. 2). A number of studies have established a correlation between synaptic load and cognitive function. Based on this, one could speculate that increased synaptic load in mice undergoing PE could indicate an improvement in cognitive function (Quirie et al. 2012; Waterhouse and Xu 2009). This is in accordance with other studies showing that treadmill exercise led to a significant increase in synaptophysin levels in the ML of the hippocampus (Chen et al. 1998). The effects of PE on synaptic plasticity is shown to be mediated by Bdnf-TrkB signaling. Indeed, using a TrkB-IgG chimera to prevent Bdnf-TrkB signaling, Vaynman and colleagues were able to prevent the positive effects of PE on synaptic density in rodents (Vaynman et al. 2004). The considerably high number and the prime location of astrocytic endfeet in the proximity of synapses enwrapping these structures enable them to mediate the

positive effects of Bdnf on synapses. Accordingly, astrocytes play a significant role in generation and maintenance of functional synapses (see Filous and Silver 2016). Indeed, ablation of astrocytes in the mouse brain led to a reduction in both DGC thickness and glutamate transporters, thus hampering the ability of these cells to remove extra glutamate released in the synaptic milieu (Cui et al. 2001). It has been shown that both chronic PE and overexpression of Bdnf can increase the levels of truncated and non-truncated TrkB receptors (Kim et al. 2015; LeMaster et al. 1999). The presence of glutamate transporters on astrocytic membranes enables them to play an important role in removing excess glutamate in the synaptic cleft, thus limiting the onset and the extent of extracellular glutamate. Increased length and area of astrocytic projections due to exercise found in this study (Fig. 2) might have significant functional implications and enable them to be more efficient in performing the crucial task of combating glutamate excitotoxicity.

Binding of Bdnf to TrkB receptors leads to phosphorylation of intracellular tyrosine kinase domain of these receptors. However, a majority of astrocytes express the truncated form of TrkB (TrkB-T1) lacking the tyrosine kinase domain (Rose et al. 2003). TrkB-T1 activation leads to the release of Ca<sup>2+</sup> from intracellular stores (Armanini et al. 1995; Bezzi et al. 2004), which is believed to play a major role in the regulation of astrocytic morphology (Ohira et al. 2005). For these reasons, we studied TrkB



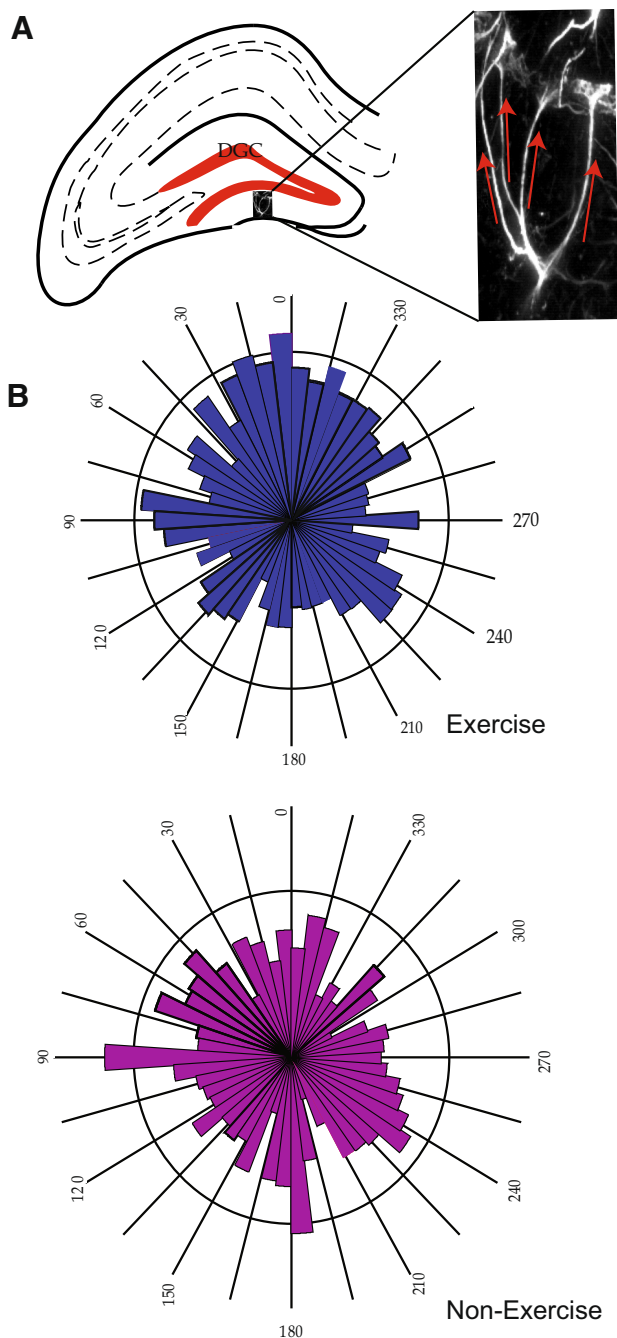


**Fig. 7** Polar histogram of the projection of GFAP-stained cells in the molecular layer of the dentate gyrus in mice undergoing physical exercise. **a** The orientation of each astrocytic projection was determined by manual tracing of projections directing toward the dentate granule cell layer ( $0^\circ$ ). **b** The figure depicts the frequency and the orientation of astrocytic projections in space. As shown here, the majority of astrocytic projections were oriented toward the dentate granule cell layer after physical exercise. Chi-square test showed a significant difference between the distributions of the two groups ( $\chi^2 = 599,13$ ,  $df = 49$ , and  $p < 0.001$ )

levels in astrocytes using an antibody that could recognize both full length and truncated forms of TrkB. While we found only a trend toward higher levels of TrkB in the ML

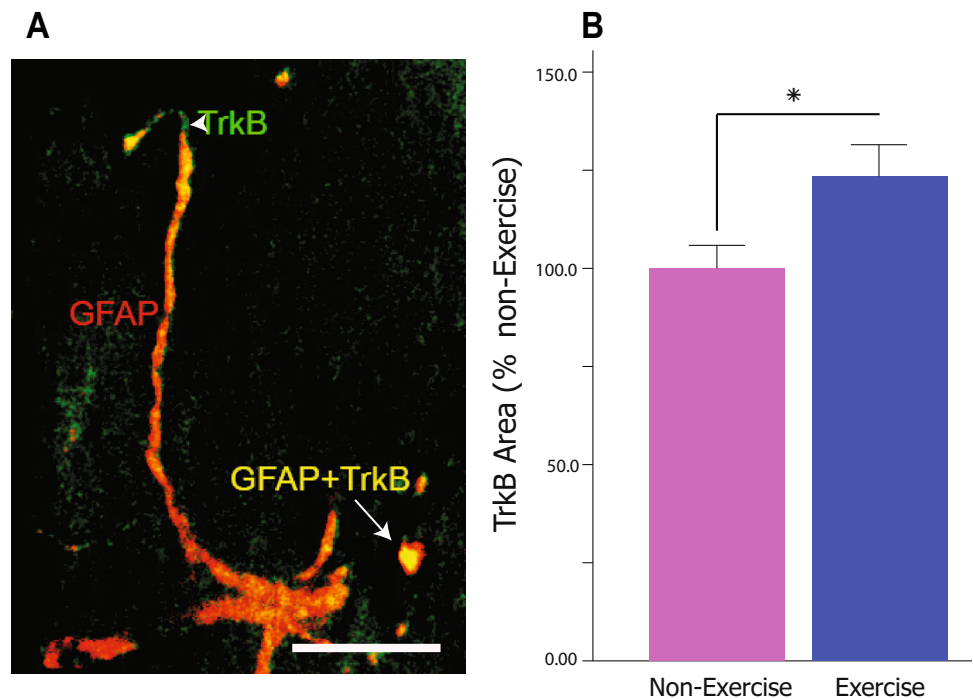
of EX mice, a significant increased levels of TrkB expression was detected in astrocytes following PE (Fig. 8). Accordingly, voluntary running in rats led to a significant increase in hippocampal Bdnf and phosphorylated TrkB (pTrkB) levels without altering total TrkB levels (Agudelo et al. 2014).

We found a significant increase in the extent of astrocyte projections in mice following exercise (Fig. 6a, b). A number of studies have established a positive relationship between the extent of astrocytes projections and well being of these cells. For instance, while Tynan and colleagues (Tynan et al. 2013) have shown that chronic stress leads to the shortening and reduction in the number of astrocytic projections in rodents, enriched environment leads to a significant increase in astrocytic projections (the number of branching point and area covered by these projections) (Diniz et al. 2010). In addition to increased extent of astrocytic projections following PE, it appears that astrocytic projections were more preferentially directed toward the DGC, i.e. a region of the hippocampus with significant increase in the synthesis and release of Bdnf following PE (Figs. 3, 7). This suggests dynamic alterations and responsiveness in astrocytic endfeet in response to physical activity.

The positive effects of PE on both Bdnf and its TrkB receptors in DG have been shown in rats undergoing PE, however; the cell type involved were not identified (Kim et al. 2015). Saur and colleagues reported an increase in the local density of GFAP-positive cells in the CA1 region of the hippocampus in mice undergoing long-term PE (Saur et al. 2014). However, quantifying the number of astrocytes in the DG, we found no significant increase in the total number of these cells following long-term PE. In addition, we were able to link morphological alterations of astrocytes to an improved Bdnf-TrkB signaling in these cells.

There are a number of studies in the literature that have dealt with the effects of PE on astrocytes. However, as highlighted by Viola and Loss (Viola and Loss 2014), important moderators like animal species, age, and the brain structure analyzed, should be taken into consideration in interpreting such results. Although a number of such studies have been done in rats (Saur et al. 2014; Mestriner et al. 2011; Matsuura et al. 2013), a few have assessed the relationship between PE and astrocytes in mice. Among them, most studies have studied the effects of PE in the context of a disease (e.g. (Matsuura et al. 2013; Kim et al. 2004; Leem et al. 2011)), in a region other than the dentate gyrus (Pereira et al. 2015; Brockett et al. 2015), or did not take into consideration Bdnf-TrkB signaling (Rodriguez et al. 2013; Latimer et al. 2011). It must be noted that our results do not necessarily link morphological alteration in astrocytes to increase Bdnf-TrkB signaling and they might be two independent phenomena. Indeed a convincing

**Fig. 8 a** A micrograph depicting colocalization between GFAP and TrkB in the DG in a non-EX mouse. **b** Quantification of the of colocalization area between GFAP and TrkB showed a significant increase in TrkB area in astrocytes in exercise mice compared with non-EX mice (non-EX =  $100.0 \pm 10.8$ ,  $n = 4$ , EX =  $137.46 \pm 10.8$ ,  $n = 6$ ,  $*p = 0.038$ ). Scale bar 10  $\mu\text{m}$



strategy would include testing the effects of exercise on astrocytes in the presence of Bdnf-TrkB signaling blockers in the DG.

Since a number of neurodegenerative disorders including AD have been linked to excess synaptic levels of glutamate (Lewerenz and Maher 2015), the positive effects of PE mediated by astrocytes might be more crucial in the context of neurodegenerative disorders than physiological conditions. Understanding the molecular mechanisms of PE has a significant implication in clinical setting. A large number of recent studies report positive effects of PE in age-dependent neurodegenerative disorders particularly AD. For instance, endurance exercise has been linked to an improvement in sleep, mini-mental state examination, and Alzheimer's disease assessment scale (Nascimento et al. 2014; Steinberg et al. 2009) in AD patients. Indeed a number of these studies showed concomitant improvement in executive functions and Bdnf in both controls and AD patients (de Andrade et al. 2013; Coelho et al. 2014).

In summary, our study suggests that astrocytes constitute an important element in mediating the positive effects of PE in the DG of the hippocampus. Furthermore, it appears that PE-induced release of Bdnf by the DG leads to a significant alteration in structure and function of astrocytes in protection against glutamate toxicity during aging and a number of neurodegenerative disorders.

**Acknowledgments** This study was supported by Grants from the Lumind/RDS and Jerome Lejeune foundations and the Alzheimer's Association. The support provided by the MIRECC and WRIISC

programs at the VA Palo Alto Health Care System is highly appreciated.

#### Compliance with ethical standards

**Conflict of interest** The authors declare that they have no conflicts of interest.

#### References

- Agudelo LZ et al (2014) Skeletal muscle PGC-1 $\alpha$ 1 modulates kynurenine metabolism and mediates resilience to stress-induced depression. *Cell* 159(1):33–45
- Armanini MP et al (1995) Truncated and catalytic isoforms of trkB are co-expressed in neurons of rat and mouse CNS. *Eur J Neurosci* 7(6):1403–1409
- Aroeira RI, Sebastiao AM, Valente CA (2015) BDNF, via truncated TrkB receptor, modulates GlyT1 and GlyT2 in astrocytes. *Glia* 63(12):2181–2197
- Barnes DE, Yaffe K (2011) The projected effect of risk factor reduction on Alzheimer's disease prevalence. *Lancet Neurol* 10(9):819–828
- Bezzi P et al (2004) Astrocytes contain a vesicular compartment that is competent for regulated exocytosis of glutamate. *Nat Neurosci* 7(6):613–620
- Brockett AT, LaMarca EA, Gould E (2015) Physical exercise enhances cognitive flexibility as well as astrocytic and synaptic markers in the medial prefrontal cortex. *PLoS One* 10(5):e0124859
- Chen YC et al (1998) Physical training modifies the age-related decrease of GAP-43 and synaptophysin in the hippocampal formation in C57BL/6J mouse. *Brain Res* 806(2):238–245
- Chowdhury TG et al (2014) Activity-based anorexia during adolescence disrupts normal development of the CA1 pyramidal cells

- in the ventral hippocampus of female rats. *Hippocampus* 24(12):1421–1429
- Coelho FG et al (2014) Acute aerobic exercise increases brain-derived neurotrophic factor levels in elderly with Alzheimer's disease. *J Alzheimers Dis* 39(2):401–408
- Cotman CW, Berchtold NC, Christie LA (2007) Exercise builds brain health: key roles of growth factor cascades and inflammation. *Trends Neurosci* 30(9):464–472
- Cui W et al (2001) Inducible ablation of astrocytes shows that these cells are required for neuronal survival in the adult brain. *Glia* 34(4):272–282
- Dang V et al (2014) Formoterol, a long-acting beta2 adrenergic agonist, improves cognitive function and promotes dendritic complexity in a mouse model of Down syndrome. *Biol Psychiatry* 75(3):179–188
- Das D et al (2015) Assessment of dendritic arborization in the dentate gyrus of the hippocampal region in mice. *J Vis Exp*. doi:10.3791/52371
- de Andrade LP et al (2013) Benefits of multimodal exercise intervention for postural control and frontal cognitive functions in individuals with Alzheimer's disease: a controlled trial. *J Am Geriatr Soc* 61(11):1919–1926
- Diniz DG et al (2010) Environmental impoverishment and aging alter object recognition, spatial learning, and dentate gyrus astrocytes. *Eur J Neurosci* 32(3):509–519
- Erickson KI, Kramer AF (2009) Aerobic exercise effects on cognitive and neural plasticity in older adults. *Br J Sports Med* 43(1):22–24
- Filous AR, Silver J (2016) Targeting astrocytes in CNS injury and disease: a translational research approach. *Prog Neurobiol* 144:173–187
- Gosset F et al (2013) Amyloid-beta peptides, Alzheimer's disease and the blood-brain barrier. *Curr Alzheimer Res* 10(10):1015–1033
- Helgager J, Huang YZ, McNamara JO (2014) Brain-derived neurotrophic factor but not vesicular zinc promotes TrkB activation within mossy fibers of mouse hippocampus in vivo. *J Comp Neurol* 522(17):3885–3899
- Hofer M et al (1990) Regional distribution of brain-derived neurotrophic factor mRNA in the adult mouse brain. *EMBO J* 9(8):2459–2464
- Jeong YJ et al (2015) 1950 MHz electromagnetic fields ameliorate Abeta pathology in Alzheimer's disease mice. *Curr Alzheimer Res* 12(5):481–492
- Kim SY et al (2004) Differential expression of phospholipase D isozymes in the hippocampus following kainic acid-induced seizures. *J Neuropathol Exp Neurol* 63(8):812–820
- Kim K et al (2015) Effects of treadmill exercise-intensity on short-term memory in the rats born of the lipopolysaccharide-exposed maternal rats. *J Exerc Rehabil* 11(6):296–302
- Kokaia Z et al (1995) Regulation of brain-derived neurotrophic factor gene expression after transient middle cerebral artery occlusion with and without brain damage. *Exp Neurol* 136(1):73–88
- Latimer CS et al (2011) Reversal of glial and neurovascular markers of unhealthy brain aging by exercise in middle-aged female mice. *PLoS One* 6(10):e26812
- Leem YH et al (2011) Chronic exercise ameliorates the neuroinflammation in mice carrying NSE/htau23. *Biochem Biophys Res Commun* 406(3):359–365
- LeMaster AM et al (1999) Overexpression of brain-derived neurotrophic factor enhances sensory innervation and selectively increases neuron number. *J Neurosci* 19(14):5919–5931
- Lewerenz J, Maher P (2015) Chronic glutamate toxicity in neurodegenerative diseases-what is the evidence? *Front Neurosci* 9:469
- Liu N et al (2012) Intracerebral transplantation of bone marrow stromal cells ameliorates tissue plasminogen activator-induced brain damage after cerebral ischemia in mice detected by in vivo and ex vivo optical imaging. *J Neurosci Res* 90(11):2086–2093
- Marlatt MW et al (2012) Running throughout middle-age improves memory function, hippocampal neurogenesis, and BDNF levels in female C57BL/6J mice. *Dev Neurobiol* 72(6):943–952
- Matsuura Y et al (2013) The effect of Anti-NGF receptor (p75 Neurotrophin Receptor) antibodies on nociceptive behavior and activation of spinal microglia in the rat brachial plexus avulsion model. *Spine (Phila Pa 1976)* 38(6):E332–E338
- Mestriner RG et al (2011) Skilled reaching training promotes astroglial changes and facilitated sensorimotor recovery after collagenase-induced intracerebral hemorrhage. *Exp Neurol* 227(1):53–61
- Mikic S, Juric DM, Carman-Krzan M (2004) Differences in the regulation of BDNF and NGF synthesis in cultured neonatal rat astrocytes. *Int J Dev Neurosci* 22(3):119–130
- Moretti L et al (2009) Radiosensitization of solid tumors by Z-VAD, a pan-caspase inhibitor. *Mol Cancer Ther* 8(5):1270–1279
- Nascimento CM et al (2014) Physical exercise in MCI elderly promotes reduction of pro-inflammatory cytokines and improvements on cognition and BDNF peripheral levels. *Curr Alzheimer Res* 11(8):799–805
- Nascimento CM et al (2015) Physical exercise improves peripheral BDNF levels and cognitive functions in mild cognitive impairment elderly with different bdnf Val66Met genotypes. *J Alzheimers Dis* 43(1):81–91
- Neeper SA et al (1996) Physical activity increases mRNA for brain-derived neurotrophic factor and nerve growth factor in rat brain. *Brain Res* 726(1–2):49–56
- Nijs J et al (2015) Brain-derived neurotrophic factor as a driving force behind neuroplasticity in neuropathic and central sensitization pain: a new therapeutic target? *Expert Opin Ther Targets* 19(4):565–576
- Ohira K et al (2005) Differential expression of the truncated TrkB receptor, T1, in the primary motor and prefrontal cortices of the adult macaque monkey. *Neurosci Lett* 385(2):105–109
- Pereira BC et al (2015) Eccentric exercise leads to glial activation but not apoptosis in mice spinal cords. *Int J Sports Med* 36(5):378–385
- Phillips C et al (2014) Neuroprotective effects of physical activity on the brain: a closer look at trophic factor signaling. *Front Cell Neurosci* 8:170
- Phillips C et al (2015a) The link between physical activity and cognitive dysfunction in Alzheimer disease. *Phys Ther* 95(7):1046–1060
- Phillips C et al (2015b) Evolution of monoaminergic system degeneration in down syndrome and Alzheimer's disease. In: Salehi A, Rafii M, Phillips C (eds) Recent advances in alzheimer research, (Volume 1), common pathogenic mechanisms between down syndrome and Alzheimer's disease. Steps toward Therapy. Bentham Science Publisher, Sharjah
- Pollock GS et al (2001) Effects of early visual experience and diurnal rhythms on BDNF mRNA and protein levels in the visual system, hippocampus, and cerebellum. *J Neurosci* 21(11):3923–3931
- Quirie A et al (2012) Comparative effect of treadmill exercise on mature BDNF production in control versus stroke rats. *PLoS One* 7(9):e44218
- Rodriguez JJ et al (2013) Enriched environment and physical activity reverse astroglial degeneration in the hippocampus of AD transgenic mice. *Cell Death Dis* 4:e678
- Rose CR et al (2003) Truncated TrkB-T1 mediates neurotrophin-evoked calcium signalling in glia cells. *Nature* 426(6962):74–78
- Rossi S et al (2005) Rabbit monoclonal antibodies: a comparative study between a novel category of immunoreagents and the corresponding mouse monoclonal antibodies. *Am J Clin Pathol* 124(2):295–302

- Salehi A et al (2006) Increased App expression in a mouse model of Down's syndrome disrupts NGF transport and causes cholinergic neuron degeneration. *Neuron* 51(1):29–42
- Salehi A et al (2009) Restoration of norepinephrine-modulated contextual memory in a mouse model of Down syndrome. *Sci Transl Med* 1(7):7ra17
- Salis AS (2013) Proactive and reactive effects of vigorous exercise on learning and vocabulary comprehension. *Percept Mot Skills* 116(3):918–928
- Saur L et al (2014) Physical exercise increases GFAP expression and induces morphological changes in hippocampal astrocytes. *Brain Struct Funct* 219(1):293–302
- Scarmeas N et al (2009) Physical activity, diet, and risk of Alzheimer disease. *JAMA* 302(6):627–637
- Scarmeas N et al (2011) Physical activity and Alzheimer disease course. *Am J Geriatr Psychiatry* 19(5):471–481
- Schwartz JP, Nishiyama N (1994) Neurotrophic factor gene expression in astrocytes during development and following injury. *Brain Res Bull* 35(5–6):403–407
- Sepulveda-Falla D et al (2011) Deposition of hyperphosphorylated tau in cerebellum of PS1 E280A Alzheimer's disease. *Brain Pathol* 21(4):452–463
- Sofroniew MV, Vinters HV (2010) Astrocytes: biology and pathology. *Acta Neuropathol* 119(1):7–35
- Song S et al (2016) Granulocyte-colony stimulating factor promotes brain repair following traumatic brain injury by recruitment of microglia and increasing neurotrophic factor expression. *Restor Neurol Neurosci* 34(3):415–431
- Steinberg M et al (2009) Evaluation of a home-based exercise program in the treatment of Alzheimer's disease: the maximizing independence in dementia (MIND) study. *Int J Geriatr Psychiatry* 24(7):680–685
- Stranahan AM, Khalil D, Gould E (2007) Running induces widespread structural alterations in the hippocampus and entorhinal cortex. *Hippocampus* 17(11):1017–1022
- Tynan RJ et al (2013) Chronic stress-induced disruption of the astrocyte network is driven by structural atrophy and not loss of astrocytes. *Acta Neuropathol* 126(1):75–91
- van Praag H (2008) Neurogenesis and exercise: past and future directions. *Neuromol Med* 10(2):128–140
- Vaynman S, Ying Z, Gomez-Pinilla F (2004) Hippocampal BDNF mediates the efficacy of exercise on synaptic plasticity and cognition. *Eur J Neurosci* 20(10):2580–2590
- Viola GG, Loss CM (2014) Letter to Editor about: "Physical exercise increases GFAP expression and induces morphological changes in hippocampal astrocytes". *Brain Struct Funct* 219(4):1509–1510
- Voss MW et al (2013) Neurobiological markers of exercise-related brain plasticity in older adults. *Brain Behav Immun* 28:90–99
- Waterhouse EG, Xu B (2009) New insights into the role of brain-derived neurotrophic factor in synaptic plasticity. *Mol Cell Neurosci* 42(2):81–89
- Yang TT et al (2015) Aging and exercise affect hippocampal neurogenesis via different mechanisms. *PLoS One* 10(7):e0132152
- Zafra F et al (1992) Regulation of brain-derived neurotrophic factor and nerve growth factor mRNA in primary cultures of hippocampal neurons and astrocytes. *J Neurosci* 12(12):4793–4799
- Zhao C et al (2006) Distinct morphological stages of dentate granule neuron maturation in the adult mouse hippocampus. *J Neurosci* 26(1):3–11